Inhomogeneous BCS-BEC crossover for trapped cold atoms in optical lattices

A. Amaricci, A. Privitera, and M. Capone

Democritos National Simulation Center, Consiglio Nazionale delle Ricerche, Istituto Officina dei Materiali (IOM) and Scuola Internazionale Superiore di Studi Avanzati (SISSA), Via Bonomea 265, 34136 Trieste, Italy

(Received 1 October 2013; revised manuscript received 2 April 2014; published 7 May 2014)

The BCS-BEC (Bose-Einstein condensation) crossover in a lattice is a powerful paradigm that describes how a superconductor deviates from the Bardeen-Cooper-Schrieffer physics as the attractive interaction increases. Optical lattices loaded with binary mixtures of cold atoms allow one to access this phenomenon experimentally in a clean and controlled way. We show that, however, the possibility to study this phenomenon in actual cold-atoms experiments is limited by the effect of the trapping potential. Real-space dynamical mean-field theory calculations show indeed that interactions and the confining potential conspire to pack the fermions in the center of the trap, which approaches a band insulator when the attraction becomes sizeable. Interestingly, the energy gap is spatially more homogeneous than the superfluid condensate order parameter. We show how this physics reflects in several observables, and we propose an alternative strategy to disentangle the effect of the harmonic potential and measure the intrinsic properties resulting from the interaction strength.

DOI: 10.1103/PhysRevA.89.053604 PACS number(s): 67.85.Lm, 03.75.Ss, 05.30.Fk, 71.10.Fd

I. INTRODUCTION

The experimental advances in handling and probing cold atoms in optical lattices open a new path towards the understanding of condensed-matter lattice models [1]. While the repulsive Fermi-Hubbard model and its Mott insulating phase [2,3] are the first natural goal because of their relation with high-temperature superconductivity, the experimental realization [4] of the attractive Fermi-Hubbard model (AHM) is an equally sensible target. The quantum simulation of the AHM has at least a twofold motivation: besides its direct significance to describe superconductors, it has been proposed as a simpler path to investigate the repulsive model, exploiting an exact mapping between the two models [5].

At low temperature the AHM describes a superfluid (SF) state, whose properties evolve continuously from a weak-coupling Bardeen-Cooper-Schrieffer (BCS) regime to a Bose-Einstein condensation (BEC) of preformed pairs as the attractive interaction is increased. The lattice counterpart of the BCS-BEC crossover [6] has been proposed as an effective description of high-temperature superconductors, and it displays significant differences with the crossover of dilute Fermi gases [7] including a pronounced maximum for intermediate pairing strength of the critical temperature, which vanishes for large attraction and a characteristic dependence on the lattice density, i.e., the number of fermions (N) per lattice site $n = N/N_s$.

The description of the lattice BCS-BEC crossover requires nonperturbative approaches, among which dynamical mean-field theory (DMFT) [8] can be particularly useful, as it correctly reproduces the exact solution both in the weak-coupling limit and in the strong-coupling limit [9,10] as well as the evolution of the normal state from which superfluidity is established [11,12]. DMFT also recovers the familiar BCS-BEC crossover for a Fermi gas in the dilute limit [13,14].

The main purpose of this paper is to study the effect of the harmonic potential which traps the atoms in cold-atom experiments on the BCS-BEC crossover. In order to take into account the broken translational invariance we need to use the so-called real-space DMFT (RDMFT), which extends the DMFT to inhomogeneous systems. The same method, with a different impurity solver (see below), has been used in Ref. [15] to identify the coexistence of SF and density waves. While our focus is different, we mention that we did not observe a tendency to density ordering, in agreement with the quantum Monte Carlo results of Ref. [16].

Our zero-temperature calculations show that increasing the attraction strength leads to a compression of the cloud, with a central region populated by two fermions of opposite spin per lattice site, as in a band insulating state, leading to a packed cloud with reduced pairing amplitude. This collapse as a function of the interaction prevents us from reaching the actual BEC regime of the AHM, where local pairs are formed, but they do not coalesce in the same region of space. Indeed, the anomalous expansion of the cloud observed in experiments [4] does not overcome this limitation, as it is essentially due to adiabatic heating [17], an effect which introduces a further obstacle to the observation of the BCS-BEC crossover by effectively increasing the temperature at fixed entropy. We characterize the hidden crossover with observables which are accessible in current cold-atom experiments, like the momentum distribution function and the single-particle spectral functions. Finally, we propose a simple way to experimentally reduce the impact of the cloud compression and unveil the "homogeneous" BCS-BEC crossover compensating the effect of the inhomogeneous potential.

The paper is organized as follows. Section II presents our model and method of solution. In Sec. III we briefly review the main results for the homogeneous model. Section IV contains the results about the same physics in the trapping potential, while Sec. V is dedicated to the spectral information. Section VI discusses the approach we propose to experimentally access the BCS-BEC crossover, and Sec. VII contains our conclusions.

II. MODEL

In all the calculations we consider an attractive Fermi-Hubbard model on a two-dimensional square optical lattice

subject to a harmonic trapping potential,

$$\mathcal{H} = -t \sum_{\langle i,j\rangle\sigma} c^{\dagger}_{i\sigma} c_{j\sigma} - U \sum_{i} n_{i\uparrow} n_{i\downarrow} + \sum_{i\sigma} V_i n_{i\sigma}, \quad (1)$$

where t is the hopping parameter between neighboring sites. The second term describes the local attractive interaction between opposite-spin fermions on the same optical lattice minimum. Finally, the last term $V_i = \frac{V_0}{2}(r_i/a)^2$ is the harmonic trapping potential, which we assumed to have spherical symmetry; a is the the lattice spacing and r_i is the distance of the site i from the trap center.

We solve Eq. (1) on a lattice of N_s sites, using RDMFT [18–20], an extension of the DMFT [8] introduced to treat inhomogeneous system. The key approximation is to assume a local, albeit site-dependent, self-energy $\hat{\Sigma}_{ij} = \hat{\Sigma}_i \delta_{ij}$. In order to deal with the superconducting phase, we recast the method in the Nambu spinor formalism [15], introducing anomalous (pair) Green's functions and self-energy components F_i and S_i, respectively. The existence of a nonzero anomalous Green's function and of a correspondent SF condensate order parameter is the fingerprint of spontaneous $U(1)$ symmetry breaking. Each local self-energy is obtained by solving an impurity problem defined by a site-dependent bath described by the function $\hat{\mathcal{G}}^{-1}_{0i}$. This latter is determined self-consistently by requiring that the single-particle Green's function G_i of each local impurity model coincides with the corresponding diagonal term of $\hat{\mathbf{G}}^{-1} = \hat{\mathbf{G}}^{-1}_0 - \hat{\Sigma}$, where

$$\left[\hat{G}^{-1}_0\right]_{ij}(z) = [z - (V_i - \mu)]\delta_{ij} - \hat{t}^{2D}_{ij}$$

are the components of the noninteracting Green's function and $\hat{t}^{2D}_{ij}$ is the tight-binding hopping matrix of the two-dimensional square optical lattice. The number of independent impurity models can be reduced by exploiting the C_{4v} symmetry of the lattice.

We solve the impurity problems at zero temperature using iterated perturbation theory (IPT) [8,21], extended to deal with the superconducting formalism [9,22]. The IPT method provides an accurate and computationally cheap solver which gives direct access to dynamical properties including the local spectral functions $\rho_i(\omega) = -\mathrm{Im}G_i(\omega)/\pi$ and hence to the local spectral gap E^g_i. This information can be experimentally accessed by a spectroscopic technique able to probe the local value of the gap (see, e.g., Ref. [23] for a cold-atom analog of the scanning tunneling microscopy used in condensed matter). We compare our calculations with local-density approximation (LDA) results where the local observables on each site are those obtained within the DMFT for a homogeneous system with the chemical potential $\mu_i = \mu - V_i$.

III. BCS-BEC HOMOGENEOUS CROSSOVER: A REMINDER

We briefly recall the main properties of the SF phase of the homogeneous Hubbard model and their evolution as a function of the coupling strength U. At zero temperature the system is always SF at every band filling $n = 1/N_s \sum_i n_i \equiv 1/N_s \sum_{i\sigma} \langle c^{\dagger}_{i\sigma} c_{i\sigma}\rangle$. At half-filling $n = 1$ an extra symmetry makes the SF degenerate with a commensurate charge density wave. The zero-temperature SF condensate order parameter $\phi = 1/N_s \sum_i \phi_i = 1/N_s \sum_i \langle c_{i\uparrow} c_{i\downarrow}\rangle$ and the spectral gap E^g monotonically increase as a function of U, while the critical temperature is an increasing function of U only for weak and moderate coupling, it reaches a maximum for intermediate coupling and eventually decreases for intermediate and large U. This reduction of T_c while the gap increases is a signature of the lattice BEC regime whose fingerprints are present also at zero temperature. The large pairing strength locks the fermions in strongly bound local pairs, moving only through virtual processes of order t^2/U (a small number if $U \gg t$), making it harder and harder to establish phase coherence over the whole system. In this regime the critical temperature is controlled by the SF stiffness, which in turn is proportional to t^2/U and decreases rapidly, as opposed to the weak-coupling regime, where the standard result $T_c \propto \phi$ is recovered. It is worth noting that, in this strong coupling regime, pairing without phase coherence results in a normal state with a pseudogap in the spectrum.

This evolution is the lattice BCS-BEC crossover, which has been proposed as a qualitative description of the doping evolution of the superconducting phase of high-temperature superconductors [24] and of other superconductors that display a "domelike" behavior as a function of a control parameter [25].

The BEC side of the crossover is characterized also by a kinetic-energy gain which stabilizes the SF state at the critical temperature, in contrast with the weak-coupling regime, where a potential-energy gain leads to the SF in agreement with the BCS theory [10].

We finally note a simple result that will be important in the following. The lattice periodicity introduces a nonmonotonic dependence of the SF properties on the density. ϕ is maximum at half-filling $n = 1$ where the system is particle-hole symmetric, and it vanishes for empty and completely filled lattices.

IV. BCS-BEC INHOMOGENEOUS CROSSOVER

In Fig. 1 we show the evolution of the density profile n_i and of the local pairing amplitude ϕ_i for increasing U along the $y_i = 0$ axis for $N = 200$ fermions on a lattice of $N_s = 29 \times 29$ sites. As pointed out in Ref. [15], defining a

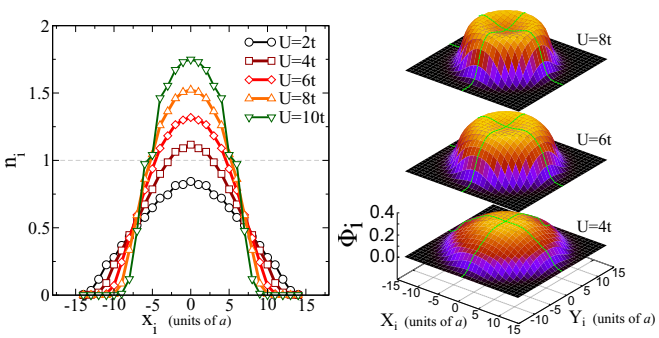

FIG. 1. (Color online) Left panel: Local density n_i profiles along the $y_i = 0$ axis of the lattice for $N = 200$ fermions, $V_0 = 0.03t$, $N_s = 29 \times 29$ sites and increasing attraction U. Right panel: Evolution of the corresponding superfluid amplitude ϕ_i surface. Data for $U = 4t$ (bottom), $U = 6t$ (center), and $U = 8t$ (top).

typical radius r_c such that $\frac{V_0}{2}(r_c/a)^2 = t$ and rescaling the density profiles in units of r_c, the results for fixed μ and increasing r_c, i.e., increasing N and decreasing V_0, collapse on the same curve. Thus our results are directly relevant for current experiments in ultracold gases as they can be easily extrapolated to actual system size and number of particles.

The density profiles for moderate and large U show that the confining potential and the interaction concur in pushing the fermions towards the trap center and in squeezing the cloud size. This effect is clearly triggered by the presence of the harmonic potential, which favors a higher occupation of the central region. In the presence of an attractive interaction, this tendency is further enhanced by the energy gain associated with doubly occupied sites. This leads, as the interaction grows, to a packing of the central region, in which most of the fermions are confined, which approaches a local density of $n = 2$ (as for a band insulator), giving rise to a more compact cloud with sharper boundaries with respect to a repulsive case, in which the interaction spreads the fermions in space.

The local SF amplitude ϕ_i (see Fig. 1) has a nontrivial evolution. For weak interaction ϕ_i is maximum at the trap center and decreases monotonously moving towards the edges of the condensate. By increasing the interaction, for $U = 6t$, the maximum at the center turns into a minimum while a shallow maximum develops at a distance from the center. By further increasing the interaction the maximum moves greater distances, while the whole pairing profile decreases.

This behavior can be qualitatively traced back to the nonmonotonic behavior of ϕ as a function of filling, which is symmetric around a maximum at half-filling. In a LDA scheme, increasing the local density beyond half-filling is therefore expected to lead to a decrease of ϕ. For our number of electrons, which would correspond to a density of $n \simeq 0.238$ in a homogeneous system, at weak coupling the cloud compression due to trap and interaction is not strong enough to raise the local density n_0 in the trap center above 1. In this case ϕ_i is maximum in the trap center and decreases monotonously as a function of the distance from the trap center. At large U instead the cloud compression becomes strong enough to have $n_0 > 1$, and, although the attraction is larger, the order parameter in the trap center is suppressed and the SF order amplitude acquires a ring shape, with a maximum amplitude around the line where the local density crosses $n_i = 1$. We anticipate that, while the SF order parameter is indeed reasonably well described by an LDA approximation, the spectral gap does not closely follow the local density, and it is much more homogeneous.

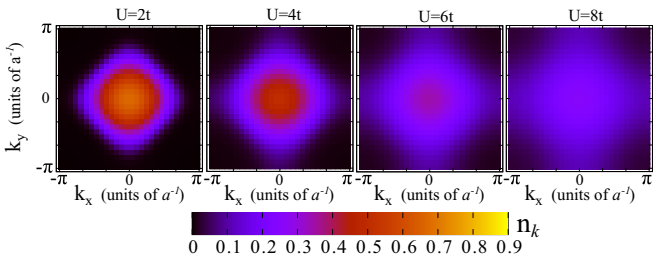

FIG. 2. (Color online) Evolution of the momentum distribution n_k as a function of the increasing attraction U. The model parameters are as in Fig. 1.

It is important to notice that, besides the peculiar spatial pattern of the pairing amplitude, the collapse of the fermionic cloud significantly reduces the all the SF properties with respect to a homogeneous system with the same interaction strength and number of fermions. This is associated with the proliferation of empty and doubly occupied sites, configurations that share a vanishing pairing amplitude. Therefore the BCS-BEC crossover we would observe in a homogeneous system is hidden by this effect, which starts already for intermediate coupling.

The same physics is reflected in the momentum distribution function $n_k = \langle c_k^\dagger c_k \rangle$, which is easily accessible in time-of-flight measurements. Our RDMFT results, shown in Fig. 2, spotlight a rapid evolution from a BCS regime, characterized by ballistic expansion of the fermions

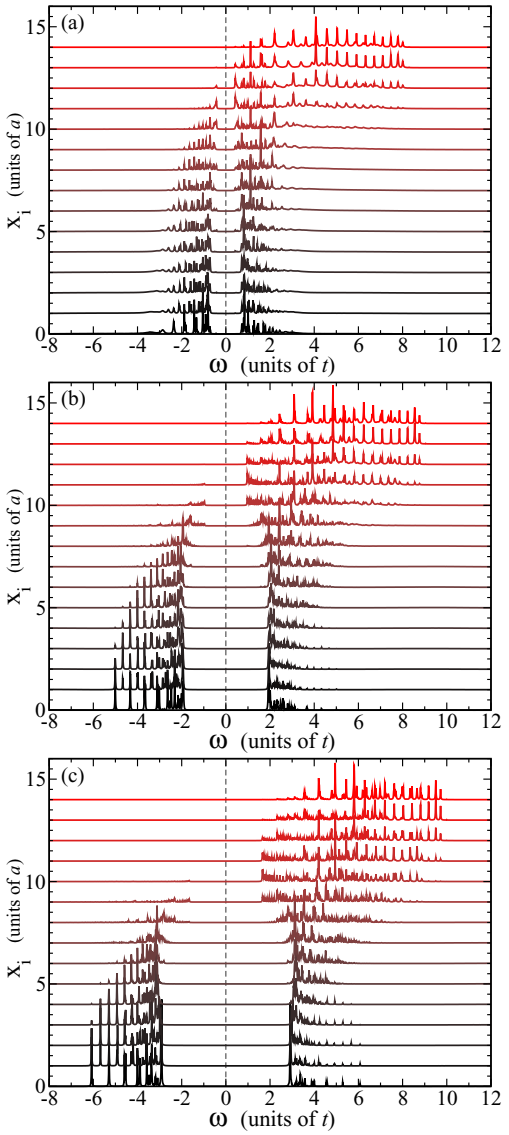

FIG. 3. (Color online) Spectral function evolution of the trapped system for $U = 4t$ (a), $U = 6t$ (b), and $U = 8t$ (c), from the trap center (bottom of each panel) to the edge (top) along the x axis ($y_i = 0$). The other model parameters are as in Fig. 1. The figure underlines the larger homogeneity of the low-energy part of the spectral functions.

and a clearly visible remnant Fermi surface to an intermediate coupling in which most fermions are gathered in the center of the trap and the momentum distribution becomes very broad while the Fermi surface is washed out by the reduction of the single-particle coherence.

V. SPECTRAL DENSITY AND ENERGY GAP

One of the most valuable features of the DMFT and related methods is that it provides direct access to dynamical properties, including the local spectral function $\rho_i(\omega) = -1/\pi \mathrm{Im} G_i(\omega^+)$, which contains the information about the excitation of the system. An inspection of these observables in our inhomoegeneous trapped system provides further information about the interplay between the interaction physics and the effect of the potential, showing that the local spectral gap E_i^g is much more homogeneous than the condensate order parameter.

In Fig. 3 we report the evolution of the local single-particle spectral function $\rho_i(\omega)$ along a cut parallel to the x axis from the trap center (bottom of each panel) to the lattice edge (top of each panel), for three different values of U. Notice that the discrete nature of the spectral function is a genuine feature due to the finite lattice and the trapping potential and it does not result from the RDMFT treatment or from numerics.

The main feature of all the plots is that the evolution of the spectral functions as we move from the center to the boundary of the trap is dominated by the change in the local density. Near the trap center, where the highest value of density is attained, the spectral density is largely concentrated below the Fermi level. This imbalance is further enhanced at a larger value of the attraction. Upon moving towards the trap boundary the local density is reduced and we observe a transfer of the spectral weight to higher energy.

The most interesting physical result is, however, that the low-energy part of the spectrum does not change much as we move along the lattice, and the energy gap E_i^g appears much more uniform than the whole spectral function. This behavior is reflected also in the observables that characterize the superfluid state.

In order to further substantiate this analysis we show in Fig. 4 the local gap E_i^g and order parameter ϕ_i as a function of the lattice site i along the x axis (the y variable is set at the center of the trap). For the sake of comparison, E_i^g is divided by U, so that it can be more closely compared with ϕ_i (in the BCS regime $E^g = U\phi$). We show for comparison (dashed lines) LDA results in which the local properties are those obtained within the DMFT for a homogeneous system with a chemical potential corrected by the local trap potential. In the inset of each figure we plot the same observables as a function of the local density.

Even if the global change in the curves going from the center to the edge of the trap may suggest that the RDMFT results are reasonably reproduced by the LDA, significant deviations appear in the most delicate border region (notice that the center of the trap hosts an essentially trivial state). As we mentioned above, the spectral gap shows the most significant deviations with respect to the LDA. E_i^g remains indeed essentially uniform in space also in the proximity of the cloud edge, while ϕ_i vanishes as predicted by the LDA. This leads to a strong deviation from the BCS proportionality between the two observables. As a matter of fact, the boundary of the cloud behaves like a phase-disordered superconductor with a finite spectral gap and no actual condensate order parameter. This bifurcation in the behavior of the gap and of the order parameter is connected to the dynamical nature of the RDMFT solution. Indeed ϕ_i can be computed as an integral of the *whole* frequency range of the anomalous Green's function, while E_i^g is extracted from the low-frequency part. Our results therefore show that the low-energy part of the spectrum is much more homogeneous than the high-energy part. We can understand this result in terms of the different natures of the two kind of excitations. Low-energy excitation are essentially delocalized in space, and they are therefore less sensitive to the local density, while the high-energy features are associated with essentially local excitation processes, which are therefore controlled by the local density.

Interestingly, a similar behavior is indeed observed in Ref. [26] in the context of chemically disordered superconductors, suggesting that the bifurcation between low- and high-energy physics can be a general explanation of the behavior of inhomogeneous superconductors independently of the nature of the underlying inhomogeneity.

VI. OPTIMIZED PROTOCOL TO DETECT THE BCS-BEC CROSSOVER

Our RDMFT solution of the AHM in a trapping potential prompts that, in order to reveal the full BCS-BEC crossover in

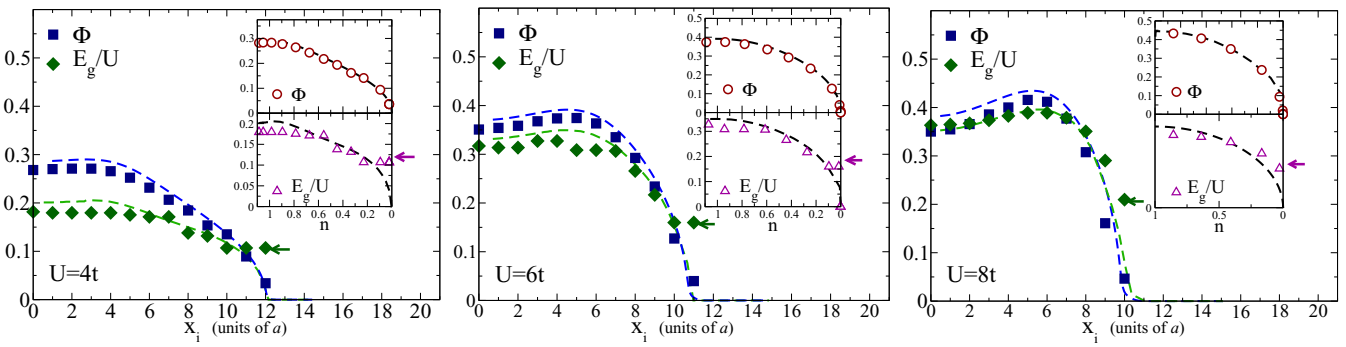

FIG. 4. (Color online) Energy gap E_i^g and order parameter ϕ_i evolution along the x axis ($y_i = 0$) for $U = 4t$ (left), $U = 6t$ (center), and $U = 8t$ (right). The other model parameters are as in Fig. 1. Insets: The order parameter ϕ_i and the gap E_i^g as a function of the density n_i. The arrows indicate the large discontinuity at the border of the cloud.

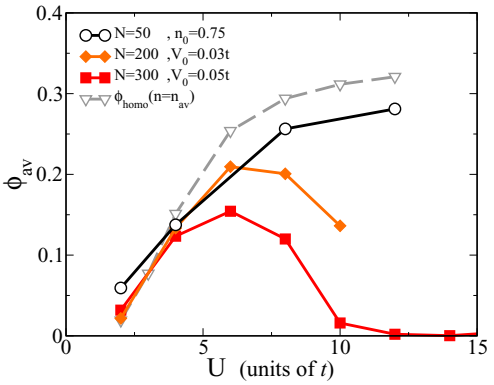

FIG. 5. (Color online) Average superfluid amplitude ϕ_{av} as a function of interaction U. Data from different protocols for the BCS-BEC crossover obtained by fixing $N = 50$ and trap center density $n_0 = 0.75$ (open circles); $N = 200$ and $V_0 = 0.03t$ (diamonds); and $N = 300$ and $V_0 = 0.05t$ (squares). Dashed line indicates the homogeneous solution with the same average density n_{av} as in the $N = 50$ and $n_0 = 0.75$ case.

a lattice, it is not sufficient to increase the interaction keeping the trapping potential fixed, instead a more careful protocol must be considered. In particular one needs to compensate the cloud compression due to the increased interaction and keep the density as uniform as possible and, most importantly, independent of U. The simplest knob we can use to this end is the strength of the trapping potential. When U increases, we can decrease V_0 and compensate for the cloud compression. As a matter of fact, it turns out that a suitable change of V_0 is sufficient to reproduce an essentially constant density pattern for a wide range of U. This compensation protocol avoids the collapse of the cloud and allows for a sensible comparison between different values of U.

In Fig. 5 we show the performance of this compensation protocol. We define the average density n_{av} and order parameter ϕ_{av} performing the average over the region with local density larger than $n_i > 0.001$ (i.e., over the whole cloud). We perform calculations for different values of U, choosing V_0 in order to keep constant the central density $n_0 = 0.75$. This simple requirement makes also the average density in the cloud n_{av} essentially constant as U goes from 2 to 12 and the whole density profile depends very weakly on U.

The success of this choice in revealing the properties of the BCS-BEC crossover is demonstrated by Fig. 5, where we compare ϕ_{av} for calculations at fixed V_0 and for fixed n_0 with a homogeneous solution for $n = n_{\mathrm{av}}$. It is apparent that calculations at fixed V_0 fail in describing the monotonic increase of ϕ_{av} as the interaction grows. On the other hand, the compensated protocol is perfectly able of reproducing the qualitative trend of the homogeneous crossover. Therefore this protocol is expected to reveal all the relevant features of the BCS-BEC crossover, including the opening of the pseudogap above the critical temperature on the BEC side.

VII. CONCLUSIONS

We have studied the two-dimensional attractive Fermi-Hubbard model in the presence of a trapping potential in order to describe fermionic atoms trapped in optical lattices. We have shown that the detection of the BCS-BEC crossover in the AHM in this system is not straightforward. Using a fixed trapping potential and increasing the value of the attractive potential U, we do not reach a proper BEC regime because the fermionic cloud collapses into a packed "band-insulating" state with two fermions per site. This physics is reflected in measurable quantities, including spectral functions, energy gaps, and momentum distribution functions. Interestingly, the energy gap is more homogeneous than the superfluid condensate order parameter and significantly deviates from the LDA. The limitations introduced by the trapping potential can be overcome by tuning the strength of the potential in order to keep the density at the center of the trap independent of the value of U. This simple choice leads to an essentially interaction-independent density pattern which allows one to recover the main features of the lattice BCS-BEC crossover. A similar protocol should also be used to study more complex situations with population [27] and/or mass [28,29] imbalance between the two fermionic species in order to reveal new exotic phases such as Sarma states and Fulde-Ferell-Larkin-Ovchinnikov superfluidity [30–32].

ACKNOWLEDGMENTS

This work is financed by EU FP7 through the ERC Starting Grant "SUPERBAD," Grant No. 240524, the LEMSUPER Project (Grant No. 283214), and the GO-FAST project (Grant Agreement No. 280555).

[1] I. Bloch, J. Dalibard, and S. Nascimbene, Nat. Phys. **8**, 267 (2012).
[2] R. Jordens, N. Strohmaier, K. Gunter, H. Moritz, and T. Esslinger, Nature (London) **455**, 204 (2008).
[3] R. Jördens, L. Tarruell, D. Greif, T. Uehlinger, N. Strohmaier, H. Moritz, T. Esslinger, L. De Leo, C. Kollath, A. Georges, V. Scarola, L. Pollet, E. Burovski, E. Kozik, and M. Troyer, Phys. Rev. Lett. **104**, 180401 (2010).
[4] L. Hackermller, U. Schneider, M. Moreno-Cardoner, T. Kitagawa, T. Best, S. Will, E. Demler, E. Altman, I. Bloch, and B. Paredes, Science **327**, 1621 (2010).
[5] A. F. Ho, M. A. Cazalilla, and T. Giamarchi, Phys. Rev. A **79**, 033620 (2009).
[6] P. Nozieres and S. Schmitt-Rink, J. Low Temp. Phys. **59**, 195 (1985).
[7] W. Zwerger, *The BCS-BEC Crossover and the Unitary Fermi Gas* (Springer-Verlag, Berlin, Heidelberg, 2012).
[8] A. Georges, G. Kotliar, W. Krauth, and M. J. Rozenberg, Rev. Mod. Phys. **68**, 13 (1996).
[9] A. Garg, H. R. Krishnamurthy, and M. Randeria, Phys. Rev. B **72**, 024517 (2005).

[10] A. Toschi, P. Barone, M. Capone, and C. Castellani, New J. Phys. **7**, 7 (2005).
[11] M. Keller, W. Metzner, and U. Schollwöck, Phys. Rev. Lett. **86**, 4612 (2001).
[12] M. Capone, C. Castellani, and M. Grilli, Phys. Rev. Lett. **88**, 126403 (2002).
[13] A. Privitera, M. Capone, and C. Castellani, Phys. Rev. B **81**, 014523 (2010).
[14] A. Privitera and M. Capone, Phys. Rev. A **85**, 013640 (2012).
[15] A. Koga, T. Higashiyama, K. Inaba, S. Suga, and N. Kawakami, Phys. Rev. A **79**, 013607 (2009).
[16] E. Assmann, S. Chiesa, G. G. Batrouni, H. G. Evertz, and R. T. Scalettar, Phys. Rev. B **85**, 014509 (2012).
[17] B. Schmidt, M. R. Bakhtiari, I. Titvinidze, U. Schneider, M. Snoek, and W. Hofstetter, Phys. Rev. Lett. **110**, 075302 (2013).
[18] R. W. Helmes, T. A. Costi, and A. Rosch, Phys. Rev. Lett. **100**, 056403 (2008).
[19] E. C. Andrade, E. Miranda, and V. Dobrosavljevic, Phys. Rev. Lett. **102**, 206403 (2009).
[20] E. Miranda and V. Dobrosavljevic, *Dynamical Mean-Field Theories of Correlation and Disorder* (Oxford University Press, London, 2012).
[21] H. Kajueter, G. Kotliar, and G. Moeller, Phys. Rev. B **53**, 16214 (1996).
[22] J. Bauer, A. C. Hewson, and N. Dupuis, Phys. Rev. B **79**, 214518 (2009).
[23] T. Gericke, P. Wurtz, D. Reitz, T. Langen, and H. Ott, Nat. Phys. **4**, 949 (2008).
[24] Q. Chen, J. Stajic, S. Tan, and K. Levin, Phys. Rep. **412**, 1 (2005).
[25] M. Capone, M. Fabrizio, C. Castellani, and E. Tosatti, Rev. Mod. Phys. **81**, 943 (2009).
[26] B. Sacepe, T. Dubouchet, C. Chapelier, M. Sanquer, M. Ovadia, D. Shahar, M. Feigelm'an, and L. Ioffe, Nat. Phys. **7**, 239 (2011).
[27] T.-L. Dao, M. Ferrero, A. Georges, M. Capone, and O. Parcollet, Phys. Rev. Lett. **101**, 236405 (2008).
[28] T.-L. Dao, A. Georges, and M. Capone, Phys. Rev. B **76**, 104517 (2007).
[29] T.-L. Dao, M. Ferrero, P. S. Cornaglia, and M. Capone, Phys. Rev. A **85**, 013606 (2012).
[30] D.-H. Kim, J. J. Kinnunen, J.-P. Martikainen, and P. Törmä, Phys. Rev. Lett. **106**, 095301 (2011).
[31] D.-H. Kim and P. Törmä, Phys. Rev. B **85**, 180508 (2012).
[32] M. O. J. Heikkinen, D.-H. Kim, and P. Törmä, Phys. Rev. B **87**, 224513 (2013).